

Multimodal virtual bronchoscopy using PET/CT images

Karl-Hans Englmeier & Marcus D. Seemann

To cite this article: Karl-Hans Englmeier & Marcus D. Seemann (2008) Multimodal virtual bronchoscopy using PET/CT images, Computer Aided Surgery, 13:2, 106-113, DOI: [10.3109/10929080801954164](https://doi.org/10.3109/10929080801954164)

To link to this article: <http://dx.doi.org/10.3109/10929080801954164>



© 2008 Informa UK Ltd All rights reserved: reproduction in whole or part not permitted



Published online: 06 Jan 2010.



Submit your article to this journal [↗](#)



Article views: 65



View related articles [↗](#)

BIOMEDICAL PAPER

Multimodal virtual bronchoscopy using PET/CT images

KARL-HANS ENGLMEIER¹ & MARCUS D. SEEMANN²

¹Institute for Biomedical and Medical Imaging, Helholz Center Munich, Munich, and ²Department of Radiology and Nuclear Medicine, University of Magdeburg, Magdeburg, Germany

(Received 30 October 2007; accepted 15 January 2008)

Abstract

Objective: To demonstrate the possibilities, advantages and limitations of virtual bronchoscopy using data sets from positron emission tomography (PET) and computed tomography (CT).

Materials and Methods: Eight consecutive patients with non-small cell lung cancer (NSCLC) underwent PET/CT. PET was performed with a glucose analog, 2-[fluorine-18]-fluoro-2-deoxy-D-glucose (¹⁸F-FDG), using a state-of-the-art full-ring Pico-3D PET scanner. CT was performed with a venous-dominant contrast-enhanced phase using a 16-slice CT scanner. The tracheobronchial system was segmented using the CT data set with an interactive threshold interval volume-growing segmentation algorithm. The primary tumors and lymph node metastases were segmented for virtual CT-bronchoscopy using the CT data set and for virtual hybrid bronchoscopy using the PET/CT data set. The structures of interest were visualized with a color-coded shaded-surface rendering method.

Results: The use of CT and virtual CT-bronchoscopy primarily facilitates visualization of the anatomical details of the tracheobronchial system and detection of anatomical/morphologic structural changes caused by disease. PET/CT and virtual hybrid bronchoscopy, or virtual PET/CT-bronchoscopy, give superior results to virtual CT-bronchoscopy because the hybrid bronchoscopy uses both the CT information and the molecular/metabolic information about the disease obtained from PET.

Conclusions: PET/CT imaging has proven to be a highly valuable oncological diagnostic modality. Virtual hybrid bronchoscopy can be performed using a low-dose CT scan or diagnostic CT. However, it is expected to improve diagnostic accuracy in identification and characterization of malignancies, verification of infections, and differentiation of viable tumor tissue from atelectases and scar tissue, as well as assessment of tumor staging and therapeutic response, and detection of early stage recurrences that are not detectable or are liable to be misjudged using virtual CT-bronchoscopy. It could also be useful as a screening examination method for patients with suspected endobronchial malignancy. Virtual hybrid bronchoscopy with a transparent color-coded shaded-surface rendering model offers a useful alternative to fiberoptic bronchoscopy, and is particularly promising for patients for whom fiberoptic bronchoscopy is not feasible, contraindicated or refused.

Keywords: Tracheobronchial system, three-dimensional visualization, image fusion, virtual endoscopy, virtual CT-bronchoscopy, virtual hybrid bronchoscopy, PET/CT, PET-CT

Introduction

Computed tomography (CT) is the standard modality for thoracic imaging and provides important information regarding the operability and prognosis of lung tumors [1, 2]. The use of thin-section helical CT for the depiction and diagnosis of endotracheal and endobronchial disease and for planning the

treatment of airway abnormalities is well established [3–7]. The increasing use of multi-detector CT (MD-CT) scanners allows the acquisition of data sets from large areas of the body with reduced slice thickness, without increasing the total scanning time required or compromising the tissue volume scanned within a given time. Although the volume

Correspondence: Karl-Hans Englmeier, Ph.D., Institute for Biomedical and Medical Imaging, Helholz Center Munich, Munich, Germany. Tel: ++49 89 3187 4148. Fax: ++49 89 3187 4243. E-mail: englmeier@gsf.de

Part of this research was previously presented at the 15th Medicine Meets Virtual Reality Conference (MMVR15) held in Long Beach, California, in February 2007.

data sets of helical CT are usually reconstructed into a large number of axial images for diagnostic interpretation, the commonly used axial image representation is not ideal for understanding complex 3D anatomy and abnormalities, and pathological findings make interpretation even more complicated [8, 9]. Numerous studies have reported that alternative reconstruction techniques are a valuable diagnostic complement to axial source images, providing quantitative and qualitative improvements in the diagnostic assessment of airway stenoses [4, 8–15]. Consequently, high-quality image data processing methods have become increasingly important in clinical practice over the last few years [16–19]. However, disease detection from CT data relies primarily on changes in anatomical structure and morphology.

Positron emission tomography (PET) facilitates the evaluation of molecular aspects and metabolic alterations that are fundamental to the detection of a wide variety of malignancies. PET imaging can be performed with different radiotracers. The most commonly used radiopharmaceutical is a glucose analog, 2-[fluorine-18]-fluoro-2-deoxy-D-glucose (^{18}F -FDG). Imaging relies on the detection of an increased rate of aerobic glycolysis. In most cancers, malignant cells are associated with increased metabolic activity. Therefore, increased uptake of ^{18}F -FDG molecules can be used to spot areas of malignancy and tumor growth. In general, the accelerated radiotracer activity can be seen before anatomical structure changes become apparent. Variable physiologic radiotracer uptake can mimic metastatic lesions, but the main difficulty with PET is the lack of an anatomical reference frame.

The combination of PET with CT can compensate for their respective disadvantages and therefore offers several advantages over PET or CT alone. In the literature, the fusion of molecular/metabolic and anatomic/morphologic information has been shown to improve diagnostic accuracy in the identification and characterization of malignancies, and the assessment of tumor stage, therapeutic response and tumor recurrence [20, 21].

The purpose of this study was to demonstrate the possibilities, advantages and limitations of clinical application of a virtual endoscopic examination using data sets from PET/CT. To this end, a transparent color-coded surface-rendered virtual hybrid bronchoscopy was used to quantitatively evaluate tumor lesions and lymph node metastases and compare the results with those from a transparent color-coded surface-rendered virtual CT-bronchoscopy.

Material and Methods

Patients

In a three-month period, eight consecutive patients (5 men and 3 women) with extended disease from a non-small cell lung cancer (NSCLC) (central $n=5$ and peripheral $n=3$) underwent PET/CT imaging from the base of the skull to the proximal thigh. The diagnostic imaging procedure was performed in the pretherapeutic tumor staging. All patients provided informed consent. The mean age \pm standard deviation of the patients was 65.6 ± 10.6 years (range: 44–78 years).

Data acquisition

Positron emission tomography (PET) data were acquired from the base of the skull to the proximal thigh with the high-count-rate lutetium oxyorthosilicate (LSO) detector full-ring Pico-3D PET scanner of a PET/CT scanner (biograph Sensation 16[®], Siemens AG, Erlangen, Germany). All patients had to have fasted for at least 6 h beforehand, and their blood glucose level had to be <120 mg/dl. A glucose analog, 2-[fluorine-18]-fluoro-2-deoxy-D-glucose (^{18}F -FDG), was used as the radiopharmaceutical. An activity of 200 ± 18 MBq was intravenously injected 60 ± 5.6 min before starting the measurements. Depending on patient height, seven to eight bed positions (4 min emission per bed position) with a 700-mm field of view (FOV) were measured. Data acquisition was performed in a cranio-caudal direction. Images were reconstructed by means of an iterative procedure (4 iterations) with ordered subsets (8 subsets). Matrix size was 128×128 .

Computed tomography (CT) data were acquired with the 16-slice CT scanner of the same PET/CT scanner (biograph Sensation 16[®]). For an optimal assessment of the gastrointestinal tract, oral administration of 1,500 ml diluted diatrizoate meglumine (Gastrografin[®] 1.5%, Schering AG, Berlin, Germany) was performed beginning 60 min before the start of the examination. An anterior-posterior scout-view was obtained for planning and determining the location of the scanning volume. All CT scans were acquired in a cranio-caudal direction. First, a low-dose examination was performed from the base of the skull to the proximal thigh. Scanning parameters were 120 kV, 20 mAs, CARE Dose, 16×0.75 -mm section collimation, 500-ms rotation time, and 15.0-mm table feed per rotation. Images were reconstructed using an increment of 2.5 mm with a 700-mm field of view (FOV) and a kernel of B30f medium smooth. Matrix size was 512×512 . After data acquisition with PET, the contrast-enhanced examination was performed.

All patients received a total of 130 ml of a nonionic contrast agent (Imeron[®] 300, Bracco ALTANA, Pharma GmbH, Konstanz, Germany) infused through an 18-gauge intravenous antecubital catheter using a biphasic contrast-enhanced protocol (85 ml at a flow rate of 3 ml/s and then 45 ml at 1.8 ml/s) plus a chaser bolus (30 ml saline with a flow rate of 1.8 ml/s) using a dual-head power injector (Missouri XD 2001[®], Ulrich Medical Technic, Ulm, Germany). A venous-dominant contrast-enhanced examination was started 80 s after intravenous contrast media injection from the base of the skull to the proximal thigh. Scanning parameters were 120 kV, 160 mAs, CARE Dose, 16×0.75 -mm section collimation, 500-ms rotation time, and 15.0-mm table feed per rotation. Axial CT images were reconstructed using an increment of 2.5 mm with a 500-mm field of view (FOV) and a kernel of B30f medium smooth. Matrix size was 512×512 .

Image postprocessing

The PET and CT data sets were automatically superimposed (MSViewer, Navigator, Siemens AG) and transferred to a high-performance LINUX cluster (HELP VR by Siemens; Amira by Mercury Computer Systems). A software package developed in-house was used to create the 3D models and perform virtual endoscopic examinations. The software program allowed highlighting of the PET and CT images of the PET/CT data sets, manual image control, and magnification of each region. For virtual CT-bronchoscopy, the tracheobronchial system and the pathological findings of the chest, mediastinum and hilar region were segmented interactively by volume-growing using the CT data sets. For virtual PET/CT-bronchoscopy, the tracheobronchial system was segmented interactively by volume-growing using the CT data sets, and the pathological findings of the chest, mediastinum and hilar region were segmented interactively by volume-growing using the PET and CT data sets. For performance of an interactive, automatic, volume-growing segmentation process, an individual threshold-based interval value for each anatomical and pathological structure had to be defined.

For the evaluation of the PET images, standardized uptake values (SUVs) were used to increase lesion detectability. Any focal tracer uptake higher than an SUV of 5 was rated as pathological tracer accumulation. Within the lung parenchyma it was classified as primary tumor, and within the mediastinum and hilar region it was classified as lymph node metastasis. For the evaluation of the CT images, lesions with a pathological

appearance within the lung parenchyma were rated as primary tumor, and lesions with a nodular shape and a diameter of more than 10 mm within the mediastinum and hilar region were staged as lymph node metastases. Only lesions for which the confidence rate was high were taken into account. The manual placement of a seed point in the central region of a structure of interest partially automated the volume-growing segmentation process. Adjoining voxels with a value within the chosen segmentation range belonging to other anatomical and pathological structures were included from the segmentation process and had to be manually removed from the segmented volume. The use of additional seed points allowed fine-tuning and greater control of the segmentation and helped to reduce the amount of segmentation leakage.

After complete segmentation, the tracheobronchial system and the malignancies of the chest, mediastinum and hilar region were color coded and displayed using a shaded-surface rendering method. Freely defined virtual light sources projected both texture and shadow contours onto this network, resulting in a realistic visual impression. The software program allowed measurements of volume and distance on any plane. The viewer allowed intraluminal visualization and examination of the tracheobronchial system in real time. Virtual CT-bronchoscopy was performed using the information from the CT data sets, and virtual PET/CT-bronchoscopy was performed using the information from the PET/CT data sets. At any time during virtual bronchoscopy, it was possible to vary the degree of transparency of the tracheobronchial system, shifting from a color-coded shaded-surface view to a transparent color-coded shaded-surface view.

Image interpretation

The transparent color-coded shaded-surface virtual CT-bronchoscopy and transparent color-coded shaded-surface virtual PET/CT-bronchoscopy were separately interpreted by a specialist (in radiology and nuclear medicine) on a high-performance LINUX cluster (HELP VR, Siemens). The reviewer knew that all patients had an NSCLC. The presence of the primary tumor and the number of mediastinal and hilar lymph node metastases were described.

Results

For this study, the routine chest data set from a whole-body PET/CT examination was used

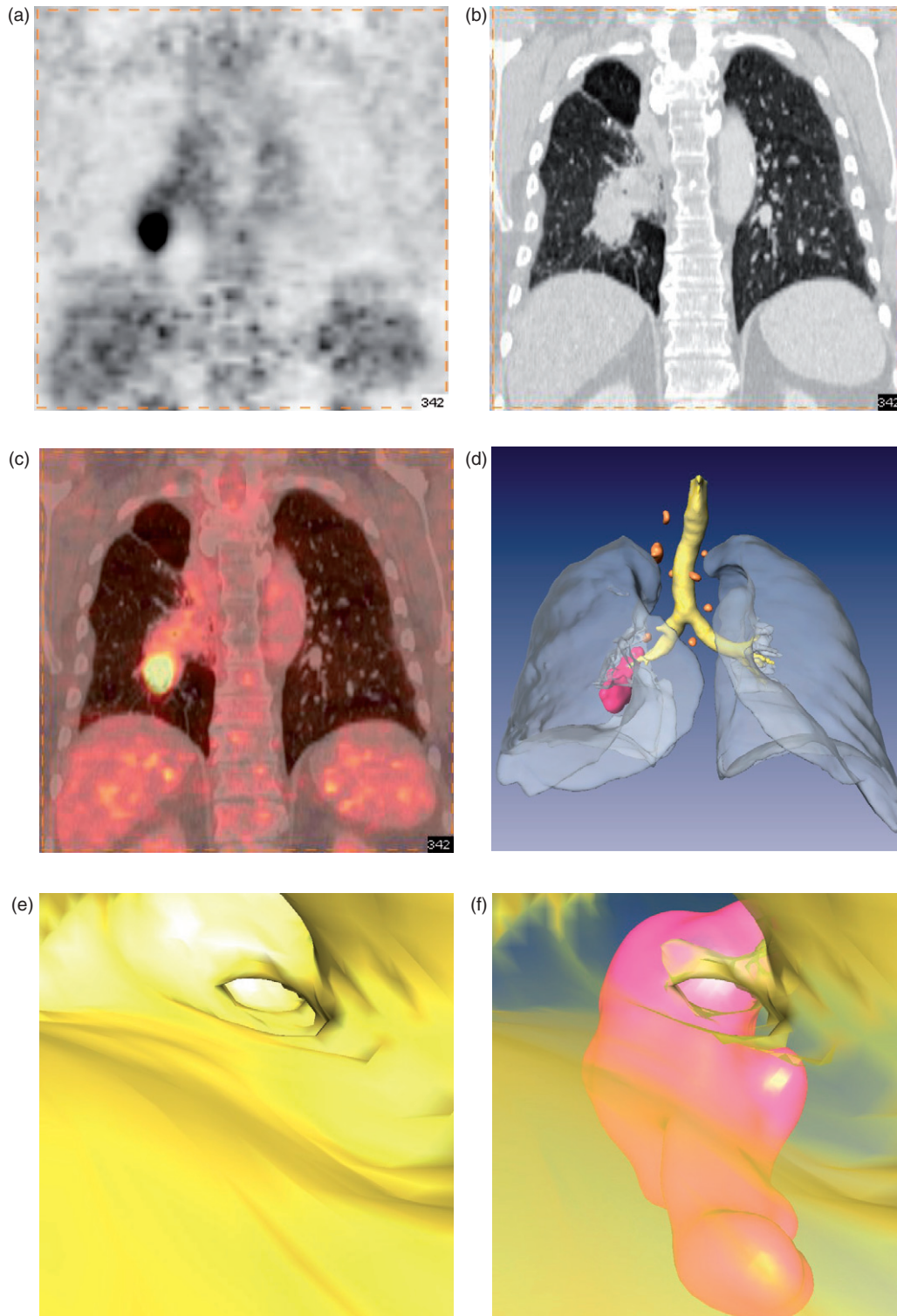


Figure 1. A 68-year-old woman with a non-small cell lung cancer (NSCLC) in the right lower lobe and mediastinal lymph node metastases. (a–c) Coronal view, showing a CT-based attenuation-corrected ^{18}F -FDG PET image (a), a venous-dominant contrast-enhanced diagnostic CT image (b), and the PET/CT image (c). ^{18}F -FDG PET and CT show the NSCLC in the caudal region of the right hilus. (d–f) Image postprocessing, showing a color-coded shaded-surface rendering model of the tracheobronchial system (yellow), the NSCLC (red) and the mediastinal lymph node metastases (orange), and a volume rendering model of the thorax (transparent, gray) (d); and virtual hybrid bronchoscopic views (e, f) of the right lower lobe bronchus, showing the NSCLC (red) in the transparent color-coded shaded-surface model (f). The tracheobronchial system was segmented using the CT data set. The bronchial carcinoma and the lymph node metastases were segmented using the PET data set. [Color version available online.]

(Figure 1a–c). The acquisition of PET emission data requires a relatively long time (several minutes) and represents an average of patient movement and respiratory and cardiac motion. The acquisition of CT data is comparatively short (a few seconds) and is therefore performed using a breath-hold technique. The deep inspiration normally used to ensure optimal expansion of the bronchial system and avoid artifacts caused by movement and breathing could not be performed. To avoid a marked discrepancy in the average position of organs, a normal expiration technique, where the patient halts respiration at the level of a normal expiration, was used during the CT data acquisition to facilitate matching of the PET and CT images.

Using high-quality interactive threshold interval volume-growing segmentation, it takes 20 min to depict the complete color-coded surface rendering model of the tracheobronchial system and the malignancies of the chest and mediastinum shown in Figure 1d. The generation of the surface-rendered images was the most operator-dependent part of the image processing, in which data can be included or excluded from the volume data set.

Virtual bronchoscopy was performed using a color-coded shaded-surface model (Figure 1e) and a transparent color-coded shaded-surface model (Figure 1f). The color-coded shaded-surface model allowed only an assessment of the intraluminal airway surface. The transparent color-coded shaded-surface rendering model of the tracheobronchial system enables the simultaneous visualization and assessment of the airways and the extraluminal pathological structures, as well as quantitative assessment of the spatial relationship between these structures.

The transparent color-coded surface-rendered virtual hybrid bronchoscopy represents the findings from the PET/CT data sets, while the transparent color-coded surface-rendered virtual CT-bronchoscopy represents the findings from the CT data set. Using both virtual bronchoscopic methods, all NSCLCs ($n=8$, 100%) were depicted (Table I). All patients showed lymph node metastases. For the detection of lymph node metastases, the transparent color-coded surface-rendered virtual hybrid bronchoscopy ($n=49$, 100%) was more sensitive than the transparent color-coded surface-rendered virtual CT-bronchoscopy ($n=43$, 87.8%), because PET showed a clearly increased tracer uptake in 6 lymph nodes that were smaller than 10 mm and were therefore not rated in the CT scan. All lymph nodes with a size greater than 10 mm in the CT scan showed increased tracer uptake in the PET scan (Table I).

Table I. Quantitative assessment of primary tumor and mediastinal lymph node metastases using virtual CT-bronchoscopy and virtual hybrid bronchoscopy ($n=8$). (Values are number of lesions detected.)

	Primary tumor metastases	Mediastinal lymph node
Virtual CT-bronchoscopy	8	43
Virtual hybrid bronchoscopy	8	49

Discussion

CT and virtual CT-bronchoscopy primarily facilitate the detection of anatomical structural changes due to disease, and the assessment of the morphological appearance of the intraluminal surface of the airways of the tracheobronchial system, airway lesions, bronchial irregularities or discrete intraluminal filling defects. The main advantage of PET is its high sensitivity in identifying cancerous areas at an early stage. In general, the accelerated radiotracer activity can be seen before anatomical structural changes become apparent. The main difficulty with PET is the lack of an anatomical reference frame. The combination of PET with CT facilitates the accurate correlation and evaluation of molecular aspects and metabolic alterations of malignancies with anatomical and morphological findings, and can compensate for the respective disadvantages of the two modalities and therefore offer several advantages. In the literature, the fusion of molecular/metabolic and anatomic/morphologic information has been shown to improve diagnostic accuracy in the identification and characterization of malignancies, and in the assessment of tumor stage, therapeutic response and tumor recurrence [20, 21]. In this study, PET/CT and virtual hybrid bronchoscopy was the most sensitive imaging procedure for detection of both primary tumors and lymph node metastases. Virtual hybrid bronchoscopy with a transparent color-coded shaded-surface rendering model of the tracheobronchial system allows individual qualitative and quantitative localization and assessment of the intraluminal airways and the adjacent extraluminal mediastinal anatomical and pathological structures, particularly for small mediastinal and hilar lymph nodes and tumors. Therefore, virtual hybrid bronchoscopy will improve diagnostic accuracy in the diagnosis of endotracheal and endobronchial diseases. This is also supported by Pasic et al. [22], who suggested that ^{18}F -FDG PET might be useful for the evaluation of early central airway lung cancer that is occult on high-resolution CT.

¹⁸F-FDG PET imaging has become an accepted and valuable diagnostic imaging tool for patients with cancer. Kamel et al. [23] reported that ¹⁸F-FDG PET is a highly valuable diagnostic tool and has a major impact on the management of patients with small cell lung cancer (SCLC), influencing initial staging, restaging after chemotherapy or radiation treatment, and management by reducing the probability of overlooking involved areas. Marom et al. [24] reported that whole-body ¹⁸F-FDG PET was significantly more accurate than thoracic CT in staging bronchogenic carcinoma. ¹⁸F-FDG PET can differentiate viable tumor tissue from atelectases and scar tissue and is therefore helpful in planning radiotherapy of bronchial carcinoma. A further advantage of PET is the sensitive detection of lymph node metastases smaller than 10 mm which are not unequivocally assessable with morphologic imaging, and whose identification thus leads to an improvement in the reference standard. The weakness of morphologic lymph node staging is the known lack of reliable criteria, since assessment can be made only on the basis of size [25]. Nevertheless, an overall lesion-based sensitivity of 100% for lymph node metastases with the combination of PET and CT is not a realistic value, because it is possible that individual metastases showed no FDG accumulation and were not seen in the morphologic imaging or not enlarged. However, lymph nodes of a size greater than 10 mm could also be caused by an inflammatory response [26]. Van Haag et al. [27] compared ¹⁸F-FDG PET and CT in early stage non-small cell lung cancer (NSCLC) and found ¹⁸F-FDG PET superior to CT for clinical staging of the mediastinum. Therefore, a more confident decision regarding stratification of patients into current treatment algorithms can be made when the decision is based on PET/CT scanning rather than the current “gold standard” of CT scanning. Although breath-holding is the standard technique for CT, it is impractical for PET. Misregistration of central lung nodules on PET and CT was determined to be 7.6 mm on average for ¹⁸F-FDG-avid lung lesions, with a tendency to be more marked in the lung base than in the middle lung zone and apex [28–30]. At the chest-abdomen interface, the discrepancy in the position of the diaphragm between the PET and CT examination results in the appearance of an infrequently severe curvilinear “cold artefact” paralleling the dome of the diaphragm in 84% of patients [31]. Therefore, adjusted breathing techniques to improve registration in the lung have been evaluated extensively [29, 30]. Goerres et al. [29, 30] reported that use of a normal expiration

technique during CT acquisition, where the patient halts respiration at the level of a normal expiration, yields the best match of PET and CT images.

Virtual hybrid bronchoscopy is a special 3D visualization technique that uses PET/CT data sets of the thorax to produce realistic simulated endobronchial views. The quality of the image postprocessing is directly affected by the PET and CT data acquisition parameters and any PET and CT limitations relating to spatial and contrast resolution [32]. Virtual hybrid bronchoscopy has several advantages over fiberoptic bronchoscopy in that it is well tolerated by patients, non-invasive, and does not require sedation. As with virtual CT-bronchoscopy, virtual hybrid bronchoscopy can pass even high-grade stenoses caused by tumors, enabling an assessment of the length of stenoses that are too severe to pass with fiberoptic bronchoscopy, and thus offering the advantage of visualizing areas beyond high-grade stenoses [4, 33]. It is always possible to correlate virtual hybrid bronchoscopic findings with the corresponding cross-sectional PET/CT images. As with virtual CT-bronchoscopy, this permits the detection and evaluation of extraluminal causes of lumen compression and facilitates differentiation of the reasons for partial and complete occlusions caused by anatomical structures (e.g., the aortic arch and tracheal cartilage), artificial changes (due to respiratory and movement artifacts resulting from cardiac and arterial pulsation and secretions) and pathological structures (caused by tumors and/or lymph nodes) [3, 5, 6, 33, 34]. Virtual hybrid bronchoscopy with a transparent color-coded shaded-surface model offers a practical alternative to fiberoptic bronchoscopy and is particularly promising for patients in whom fiberoptic bronchoscopy is not feasible, contraindicated or refused. It could be used as a complementary procedure to fiberoptic bronchoscopy in the evaluation of airway stenosis, guidance of transbronchial bronchoscopic intervention biopsy (especially in small tumors and lymph nodes), short-term monitoring in cases of primary suspect findings in fiberoptic bronchoscopy, and screening of airways for endobronchial malignancy in patients with a low clinical suspicion, e.g., young patients presenting with either infection or haemoptysis. Furthermore, virtual hybrid bronchoscopy could be an important tool in the pre-operative clarification of operability, as well as in the precise individual planning, simulation, and training of the appropriate operative technique and in the development of surgical, interventional and palliative therapies. It is potentially very useful in tumor aftercare, in detecting an early stage of recurrence, for follow-up examination of surgical,

interventional and palliative therapy, and in alternative approaches such as endoscopic laser and cryotherapy, dilation, application, after-loading and so on.

The disadvantages of virtual hybrid bronchoscopy are derived from the PET and CT technology. Any limitations of PET and CT in terms of spatial and contrast resolution directly affect the quality of the image processing methods [32]. A significant disadvantage is the radiation exposure required for scanning the PET and CT data sets, which is especially dependent upon the CT parameters chosen. As with virtual CT-bronchoscopy, distally located portions of the bronchial system can only be evaluated with virtual hybrid bronchoscopy using special threshold intervals, and they must be free of viscous secretions or coagulated blood [33]. A further disadvantage of virtual hybrid bronchoscopy is the inability to reproduce specific bronchoscopic findings, especially those portraying the mucosal surface and accurately depicting changes in color and friability of bronchial mucosal abnormalities [4, 5, 33]. Like virtual CT-bronchoscopy, virtual hybrid bronchoscopy cannot be used to obtain specimens for further cytological, microbiological or histological clarification [33]. Detailed and systematic studies are necessary to clearly define the value and clinical impact of this postprocessing technology.

Conclusions

PET/CT imaging is a highly valuable oncological diagnostic modality and will probably become very important for use in cancer screening. A PET/CT scanner offers the capability for accurate correlation of molecular/metabolic aspects of the disease and anatomical/morphological findings, and provides a clear improvement in diagnostic accuracy by combining two already excellent modalities. The increasing use of PET/CT scanners with incorporated MD-CT scanners allows the acquisition of high-quality CT data for image postprocessing and the performance of virtual hybrid endoscopy with the same data set. We have specifically highlighted its use in the visualization and assessment of the tracheobronchial system and pathological changes of the chest. The CT component will primarily provide anatomical details of the tracheobronchial system and morphological structural changes due to disease, while the PET component will identify lesions with the highest radiotracer uptake. Virtual hybrid bronchoscopy with a transparent, color-coded, shaded-surface rendering model offers new perspectives and can

be performed using a low-dose CT scan or diagnostic CT. It is expected to increase diagnostic accuracy in the detection of endotracheal/endo-bronchial, submucosal or peribronchial extension and discrete infiltrations, and mediastinal lymph node metastases; the differentiation of viable tumor tissue from atelectases and scar tissue; and the verification of infections that are not detectable or are liable to be misjudged with virtual CT-bronchoscopy.

References

1. Seemann MD, Seemann O, Dienemann H, Schalthorn A, Prime G, Fink U. Diagnostic value of chest radiography, computed tomography and tumour markers in the differentiation of malignant from benign solitary pulmonary lesions. *Eur J Med Res* 1999;4:313–327.
2. Seemann MD, Seemann O, Luboldt W, Bonél H, Sittek H, Dienemann H, Staebler A. Differentiation of malignant from benign solitary pulmonary lesions using chest radiography, spiral CT and HRCT. *Lung Cancer* 2000; 29:105–124.
3. Henschke CI, Davis SD, Auh Y, Romano P, Westcott J, Berkmen YM, Kazam E. Detection of bronchial abnormalities: comparison of CT and bronchoscopy. *J Comput Assist Tomogr* 1987;11:432–435.
4. McAdams HP, Palmer SM, Erasmus JJ, Patz EF, Connolly JE, Goodman PC, DeLong DM, Tapson VF. Bronchial anastomotic complications in lung transplant recipients: virtual bronchoscopy for noninvasive assessment. *Radiology* 1998;209:689–695.
5. Naidich DP, Lee JJ, Garay SM, McCauley DI, Aranda CP, Boyd AD. Comparison of CT and fiberoptic bronchoscopy in the evaluation of bronchial disease. *Am J Roentgenol* 1987;148:1–7.
6. Naidich DP, Harkin TJ. Airways and lung: correlation of CT with fiberoptic bronchoscopy. *Radiology* 1995; 197:1–12.
7. Zeiberg AS, Silverman PM, Sessions RB, Troost TR, Davros WJ, Zeman RK. Helical (spiral) CT of the upper airway with three-dimensional imaging: technique and clinical assessment. *Am J Roentgenol* 1996;166: 293–299.
8. Seemann MD, Seemann O, Bonél H, Suckfüll M, Englmeier KH, Naumann A, Allen CM, Reiser MF. Evaluation of the middle and inner ear structures: comparison of hybrid rendering, virtual endoscopy and axial 2D source images. *Eur Radiol* 1999;9:1851–1858.
9. Seemann MD, Gebicke K, Luboldt W, Albes JM, Vollmar J, Schaefer JF, Beinert T, Englmeier KH, Bitzer M, Claussen CD. Hybrid 3-D rendering of the thorax and surface-based virtual bronchoscopy in surgical and interventional therapy control. *Fortschr Röntgenstr* 2001;173: 650–657.
10. Kauczor HU, Wolcke B, Fischer B, Mildenerger P, Lorenz J, Thelen M. Three-dimensional helical CT of the tracheobronchial tree: evaluation of imaging protocols and assessment of suspected stenoses with bronchoscopic correlation. *Am J Roentgenol* 1996;167:419–424.
11. Lacrosse M, Trigaux JP, van Beers BE, Weynants P. 3D spiral CT of the tracheobronchial tree. *J Comput Assist Tomogr* 1995;19:341–347.

12. Lee KS, Yoon JH, Kim TK, Kim JS, Chung MP, Kwon OJ. Evaluation of tracheobronchial disease with helical CT with multiplanar and three-dimensional reconstruction: correlation with bronchoscopy. *RadioGraphics* 1997;17:555–567.
13. Newmark GM, Conces DJ, Kopecky KK. Spiral CT evaluation of the trachea and bronchi. *J Comput Assist Tomogr* 1994;18:552–554.
14. Quint LE, Whyte RI, Kazerooni EA, Martinez FJ, Cascade PN, Lynch JP III, Orringer MB, Brunsting LA III, Deeb GM. Stenosis of the central airways: evaluation by using helical CT with multiplanar reconstructions. *Radiology* 1995;194:871–877.
15. Seemann MD, Claussen CD. Hybrid 3D visualization of the chest and virtual endoscopy of the tracheobronchial system: possibilities and limitations of clinical application. *Lung Cancer* 2001;32:237–246.
16. Englmeier KH, Haubner M, Löscher A, Eckstein F, Seemann MD, van Eimeren W, Reiser MF. Hybrid rendering of multidimensional image data. *Meth Inform Med* 1997;36:1–10.
17. Seemann MD, Englmeier KH, Haubner M, Minx C, Luboldt W, Heuck A, Reiser MF. Hybrid rendering of the cervico-cranial arteries using spiral computed tomography. *Eur J Med Res* 1998;3:177–181.
18. Seemann MD, Seemann O, Englmeier KH, Allen CM, Haubner M, Reiser MF. Hybrid rendering and virtual endoscopy of the auditory and vestibular system. *Eur J Med Res* 1998;3:515–522.
19. Seemann MD, Seemann O, Luboldt W, Gebicke K, Prime G, Claussen CD. Hybrid rendering of the chest and virtual bronchoscopy. *Eur J Med Res* 2000;5:431–437.
20. Seemann MD. PET/CT: fundamental principles. *Eur J Med Res* 2004;9:241–246.
21. Seemann MD. Whole-body PET/MRI: the future in oncological imaging. *Technol Cancer Res Treat* 2005;4:577–582.
22. Pasic A, Brox HA, Comans EF, Herder GJ, Risse EK, Hoekstra OS, Postmus PE, Sutudja TG. Detection and staging of preinvasive lesions and occult lung cancer in the central airways with 18F-fluorodeoxyglucose positron emission tomography: a pilot study. *Clin Cancer Res* 2005;11:6186–6189.
23. Kamel EM, Zwahlen D, Wyss MT, Stumpe KD, von Schulthess GK, Steinert HC. Whole-body (18)F-FDG PET improves the management of patients with small cell lung cancer. *J Nucl Med* 2003;44:1911–1917.
24. Marom EM, McAdams HP, Erasmus JJ, Goodman PC, Culhane DK, Coleman RE, Herndon JE, Patz EF Jr. Staging non-small cell lung cancer with whole-body PET. *Radiology* 1999;212:803–809.
25. Bollen EC, Goei R, van 't Hof-Grootenboer BE, Versteeg CW, Engelshove HA, Lamers RJ. Interobserver variability and accuracy of computed tomographic assessment of nodal status in lung cancer. *Ann Thorac Surg* 1994;58:158–162.
26. Imdahl A, Jenkner S, Brink I, Nitzsche E, Stelben E, Moser E, Hasse J. Validation of FDG positron emission tomography for differentiation of unknown pulmonary lesions. *Eur J Cardiothorac Surg* 2001;20:324–329.
27. Van Haag DW, Follette DM, Roberts PF, Shelton D, Segel LD, Taylor TM. Advantages of positron emission tomography over computed tomography in mediastinal staging of non-small cell lung cancer. *J Surg Res* 2002;103:160–164.
28. Cohade C, Osman M, Marshall LN, Wahl RN. PET-CT: accuracy of PET and CT spatial registration of lung lesions. *Eur J Nucl Med Mol Imaging* 2003;30:721–726.
29. Goerres GW, Kamel E, Heidelberg TN, Schwitter MR, Burger C, von Schulthess GK. PET-CT image co-registration in the thorax: influence of respiration. *Eur J Nucl Med Mol Imaging* 2002;29:351–360.
30. Goerres GW, Kamel E, Seifert B, Burger C, Buck A, Hany TF, von Schulthess GK. Accuracy of image coregistration of pulmonary lesions in patients with non-small cell lung cancer using an integrated PET/CT system. *J Nucl Med* 2002;43:1469–1475.
31. Osman MM, Cohade C, Nakamoto Y, Wahl RL. Respiratory motion artifacts on PET emission images obtained using CT attenuation correction on PET-CT. *Eur J Nucl Med Mol Imaging* 2003;30:603–606.
32. Seemann MD. Human PET/CT scanners: feasibility for oncological in vivo imaging in mice. *Eur J Med Res* 2004;9:468–472.
33. Fleiter T, Merkle EM, Aschoff AJ, Lang G, Stein M, Görlich J, Liewald F, Rilinger N, Sokiranski R. Comparison of real-time virtual and fiberoptic bronchoscopy in patients with bronchial carcinomas: opportunities and limitations. *Am J Roentgenol* 1997;169:1591–1595.
34. Seemann MD, Heuschmid M, Vollmar J, Kuettner A, Schober W, Schaefer JF, Bitzer M, Claussen CD. Virtual bronchoscopy: comparison of different surface rendering models. *Technol Cancer Res Treat* 2003;2:273–279.